Intermetallics 38 (2013) 4–8

Contents lists available at SciVerse ScienceDirect

Intermetallics

journal homepage: www.elsevier.com/locate/intermet

Martensitic transformation behaviors of rapidly solidified Ti–Ni–Si alloys

Yeon-wook Kim*

Department of Advanced Materials, Keimyung University, 1000 Shindang-dong, Dalseo-gu, Daegu 704-701, Republic of Korea

ARTICLE INFO

Article history:
Received 5 September 2012
Received in revised form
27 November 2012
Accepted 12 February 2013
Available online 16 March 2013

Keywords:
A. Nanostructured intermetallics
B. Martensitic transformations
C. Rapid solidification processing
F. Diffraction

ABSTRACT

R phase transformation has been very attracting attention by extremely small temperature hysteresis in comparison with B2 → B19′ martensitic transformation of Ti–Ni binary alloys. A few percent of Ni in $Ti_{50}Ni_{50}$ alloy was substituted by Si, in this study, because it is possible that both B19′ phase and R phase are affected by addition of this third element. $Ti_{50}Ni_{49}Si_1$ and $Ti_{50}Ni_{47}Si_3$ alloy ribbons were prepared by melt spinner. Their microstructures and martensitic transformation behaviors were investigated by means of optical microscopy, X-ay diffraction and differential scanning calorimetry. The $Ti_{50}Ni_{49}Si_1$ alloy ribbon was consisted of B2 and Ti_2Ni phase, while the $Ti_{50}Ni_{47}Si_3$ alloy ribbon was fully an amorphous. Then the crystallization temperature of the amorphous ribbons was measured to be 537 °C. Any martensitic transformation behaviors in the as-spun $Ti_{50}Ni_{49}Si_1$ alloy ribbons did not appear in the temperature range examined in this study because the martensitic transformation temperature was suppressed by the formation of Ti_2Ni phase. The amorphous ribbon was annealed at the crystallization temperature. It was found that any Ti_2Ni precipitates were not found and two-stage transformation of B2 –R–B19′ occurred in the crystallized $Ti_{50}Ni_{47}Si_3$ alloy ribbons. The martensitic transformation start temperature (R_s) of the $Ti_{50}Ni_{47}Si_3$ alloy ribbon annealed at 537 °C for 5 min was 24 °C and the temperature hysteresis associated with the B2–R transformation was about 2 °C.

1. Introduction

Ti–Ni based alloys are well known for the functional materials not only as shape memory alloys with high strength and ductility but also as those exhibiting unique physical properties such as pre-transformation behaviors, which are enriched by various martensitic transformations. There are three distinct types of martensitic transformations in Ti–Ni based alloys. It has to be noticed that all alloys have a tendency to transform from B2 (cubic) to B19′ (monoclinic) martensite in Ti–Ni based alloys, and in fact for the solution-treated binary Ti–Ni binary alloys the transformation occurs from B2 to B19′ directly [1,2]. However, the second type of transformation is obtained when Ni is substituted by Cu in a binary Ti–Ni alloy [3,4]. In this case the transformation occurs in two steps, B2 → B19 → B19′, on cooling. The martensite upon the first transformation is called B19 (orthorhombic), and the second transformation represents the one from B19 to B19′. Next the third type of transformation is called R phase transformation [5,6], since the product phase was considered to be triclinic. Furthermore this R phase transformation was considered to be a pre-martensitic behavior (precursor effect) prior to the subsequent martensitic transformation of R–B19′. But it is now established that it is a martensitic transformation itself, which competes with the subsequent martensitic transformation.

R phase transformation has been very attracting attention by extremely small temperature hysteresis in comparison with the martensitic transformation B2 → B19′ of Ti–Ni binary alloys [7]. There are two cases, in which the R-phase transformation occurs: (1) Ni-rich Ti–Ni alloys are aged at proper temperatures to cause the precipitation of Ti_3Ni_4 phase and (2) heat-treatment of Ti–Ni alloys after cold working to create rearranged dislocation structures. In these cases, both R-phase and B19′ are affected by (1) stress field of precipitates and (2) stress field of dislocations, respectively [8]. However, the effect for B19′ phase is larger than that for R phase, and thus make the transformation temperatures of both phases separable. Recently, rapid solidification method was reported to induce the B2–R transformation in Ti–Ni alloys and this was attributed to an introduction of crystallographic defects such as dislocations by rapid solidification [9]. Generally there are four advantages of rapid solidification over the slower conventional solidification techniques. These are an ability to form metastable phases, increasing the solubility above the equilibrium solubility, decreasing the segregation of additions, and refining the microstructure. It is considered that all of these effects have been

* Tel./fax: +82 53 580 5547.
E-mail address: ywk@kmu.ac.kr.

0966-9795/$ – see front matter © 2013 Elsevier Ltd. All rights reserved.
http://dx.doi.org/10.1016/j.intermet.2013.02.011

attempted to change martensitic transformation behaviors by the rapid solidification process.

In this study, a few percent of Ni in $Ti_{50}Ni_{50}$ alloy was substituted by Si. Even though martensitic transformation behaviors of Ti–Ni–Si alloys have not been studied well, it is possible that both B19′ and R martensitic phase are affected by this third element. Furthermore, Ti–Ni–Si alloy ribbons were prepared to study rapid solidification effects on the martensitic transformation. Especially, when an extremely thin ribbon was prepared by melt spinner to achieve the highest cooling rate, the ribbon could solidify as amorphous phase. It was reported that the martensitic transformation behaviors could be controlled without chemical compositions by means of microstructural modification [10]. By proper annealing, therefore, the melt-spun amorphous ribbons may be crystallized to achieve the superior shape memory characteristics. The martensitic transformation behaviors of the crystallized Ti–Ni–Si ribbons were investigated, and then results obtained were compared with those from as-spun ribbons.

2. Experimental procedure

Ti–Ni–Si alloy ingots with nominal composition of $Ti_{50}Ni_{49}Si_1$ and $Ti_{50}Ni_{47}Si_3$ (at.%) were prepared from high purity elements of nickel, silicon and sponge titanium by arc melting in a water-cooled Cu hearth, then poured into a tube-type mold by vacuum injection to make a rod-type specimen. The alloys were re-melted five times under the high purity of argon atmosphere to ensure the homogeneity before pouring. A part of the rods was used for fabricating thin ribbons by melt spinner. The alloy rod was placed into quartz crucible of internal diameter 10 mm. The chamber of the melt spinning system had been evacuated to less than 1×10^{-3} Pa before re-melting. When the melt temperature reached the expected temperature, it was ejected through the nozzle with a circular shaped orifice on the outer surface of the rotating quenching wheel made of copper. The diameter of the orifice was 0.5 mm, the ejection pressure was 40 kPa and distance from the tip of the nozzle to the wheel surface was 300 μm throughout the study. The angular speed of quenching wheel was recorded by a tachometer and the temperature of the melt was measured by a non-contacting infrared thermometer.

Microstructures of cross-section and surface of the alloy ribbons were examined by optical microscopy (OM) after etching in a solution of H_2O:HCl:H_2O_2 (3:2:1). Crystallization temperature of amorphous ribbons was determined by thermo-gravimetric analysis (TGA). In order to study the martensitic transformation behaviors of the crystallized ribbons, the differential scanning calorimetries (DSC) measurements had been performed at heating and cooling rate of 10 °C/min using TA Instrument DSC-2010. The crystal structures of the ribbons were analyzed by X-ray diffraction (XRD) using CuK_α radiation.

3. Results and discussion

Fig. 1(a) and (b) shows optical micrographs of rapidly solidified $Ti_{50}Ni_{49}Si_1$ and $Ti_{50}Ni_{47}Si_3$ alloy ribbons, respectively. When the ribbons were fabricated at the wheel velocities of 55 m/s and the melt temperature of 1500 °C by the melt spinner, their thickness was about 25 μm. These operating parameters are the extreme conditions to fabricate the continuous ribbons in the melt spinning system that is used in this study. It is observed that the typical microstructure of melt-spun ribbons is the columnar structure as shown in Fig. 1(a). Because of the contact of the melt with the quenching wheel during high speed casting of melt spinning system, the heat would be extracted to the direction of the wheel during solidification so that the ribbon consisted of long grains

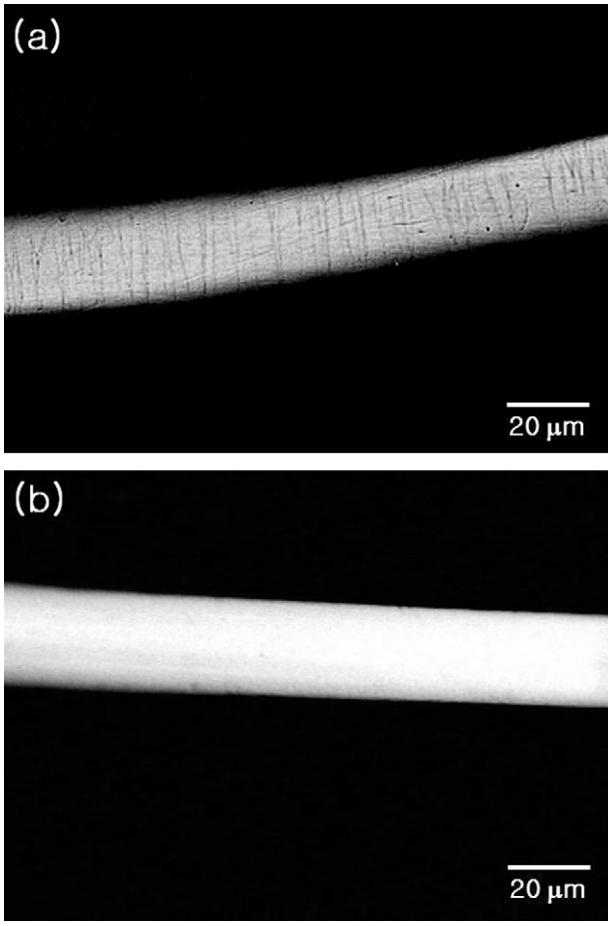

Fig. 1. Optical micrographs of (a) $Ti_{50}Ni_{49}Si_1$ and (b) $Ti_{50}Ni_{47}Si_3$ ribbons prepared by the melt spinner.

crystallographically oriented with their columnar directions normal to the surface, which were the reverse direction of the heat-extraction. However, any kinds of features were not found in the microstructure of $Ti_{50}Ni_{47}Si_3$ ribbon as shown in Fig. 1(b). Fig. 2(a) and (b) shows XRD patterns corresponding to Fig. 1(a) and (b), respectively. The diffraction peaks corresponding to the B2 and Ti_2Ni phase appear in the XRD patterns of as-spun $Ti_{50}Ni_{49}Si_1$ alloy ribbons, while the as-spun $Ti_{50}Ni_{47}Si_3$ ribbon is fully an amorphous. This result is reflecting that the glass forming ability is increased abruptly by addition of Si in Ti–Ni–Si alloys.

Fig. 3 is a DSC curve of as-spun $Ti_{50}Ni_{49}Si_1$ ribbons. Any DSC peaks of martensitic transformations are not found in the temperature range (−100 ∼ 100 °C) examined in this work, even though the ribbons solidified as crystalline phases (B2 + Ti_2Ni) as shown in Fig. 2(a). According to Nagarajan and Chattopadhyay [11,12], metastable liquidus temperature of Ti_2Ni phase decreased abruptly with increasing Ni content. This means that larger supercooling is needed for inducing Ti_2Ni phase by suppressing the nucleation of TiNi phase with increasing the Ni content. Smaller supercooling may be needed for inducing Ti_2Ni phase in $Ti_{50}Ni_{49}Si_1$ alloy ribbons than Ti–Ni binary alloys, because the melting temperature of TiNi phase decreases by substituting Ni for Si [13]. It was also reported that Si which replaced Ti promoted the nucleation of Ti_2Ni phase [11]. Therefore, Ti_2Ni phase was formed in $Ti_{50}Ni_{49}Si_1$ alloy ribbons as shown in Fig. 2(a), even though it has been reported that Ti_2Ni phase was not formed in $Ti_{50}Ni_{50}$ alloy ribbons [14]. The Ti content in B2 matrix of $Ti_{50}Ni_{49}Si_1$ ribbons must be depleted by the formation of Ti_2Ni phase. The B2 phase is an